ELSEVIER

Journal of Photochemistry and Photobiology A: Chemistry 116 (1998) 109–118

Journal of Photochemistry and Photobiology A:Chemistry

Alkyl-dependent photochemistry of [Ru(I)(R)(CO)$_2$(α-diimine)]: homolysis of the Ru–R bond for R = Bz and isomerisation for R = Me

Cornelis J. Kleverlaan, Derk J. Stufkens *

Anorganisch Chemisch Laboratorium, Institute of Molecular Chemistry, Universiteit van Amsterdam, Nieuwe Achtergracht 166, 1018 WV Amsterdam, The Netherlands

Received 9 January 1998; accepted 27 April 1998

Abstract

The complexes *trans,cis-* and *cis,cis*-[Ru(I)(Me)(CO)$_2$(α-diimine)] and *trans,cis*-[Ru(I)(Bz)(CO)$_2$(α-diimine)] (α-diimine = 4,4′-dimethyl-2,2′-bipyridine (bpy′), *N,N′*-di-isopropyl-1,4-diazabutadiene (*i*Pr-DAB)) are the subject of a photochemical study. Replacement of R = Me by R = Bz results in a dramatic change in the photochemical behaviour of the *trans,cis*-complexes. A photoisomerisation is observed for the complex *trans,cis*-[Ru(I)(Me)(CO)$_2$(bpy′)], whereas irradiation of *trans,cis*-[Ru(I)(Bz)(CO)$_2$)(α-diimine)] results in the formation of [Ru(I)$_2$(CO)$_2$)(α-diimine)]. According to the nanosecond transient absorption spectra, the primary photoprocess of both *trans,cis-* and *cis,cis*-[Ru(I)(Me)(CO)$_2$(bpy′)] is loss of CO, whereas the corresponding complexes *trans,cis*-[Ru(I)(Bz)(CO)$_2$(α-diimine)] (α-diimine = bpy′ and *i*Pr-DAB) undergo homolysis of the Ru–Bz bond. This dependence of the primary photoprocess on R is ascribed to a crossing to different reactive excited states after occupation of a nonreactive ^{1}XLCT state. For R = Me this state is proposed to have LF character, for R = Bz it is most probably the $^3\sigma\pi^*$ state.

Keywords: Ruthenium–alkyl complexes; Carbonyls; Photochemistry; Radicals; Isomerisation

1. Introduction

Most investigations of excited state properties of d^6-transition metal α-diimine complexes have been concerned with [Ru(bpy)$_3$]$^{2+}$ [1–3] and the organometallic complexes [Re(L)(CO)$_3$(bpy)]$^{n+}$ (n = 0,1) [4–8]. These complexes possess rather long-lived metal-to-ligand charge transfer (MLCT) states, and can therefore act as photosensitizers for intra- and intermolecular energy and electron transfer processes. The photophysical and photochemical properties of the Re-complexes depend on the α-diimine, and in particular on L. The related complexes [Ru(L)(L′)(CO)$_2$(α-diimine)] offer the opportunity to influence the excited state properties even more, since both L and L′ can be varied. For the complexes [Re(X)(CO)$_3$(α-diimine)] [9] and [Ru(X)(R)-(CO)$_2$(α-diimine)] [10,11] replacement of X = Cl$^-$ by I$^-$ changes the character of the excited state from MLCT to XLCT (halide to α-diimine charge transfer). In the case that L of [Re(L)(CO)$_3$(bpy)]$^{n+}$ represents an oxidizable donor molecule, MLCT excitation is followed by an intramolecular electron transfer from L to the metal, resulting in [Re^{I}(L$^+$)(CO)$_3$(bpy$^-$)]$^+$ as the lowest excited state [7]. From such an excited state the complex normally decays to the ground state without decomposition unless L represents a metal fragment or alkyl ligand. The excited state properties of quite a few such metal–metal and metal–alkyl bonded Mn, Re, and Ru complexes, viz. [(L$_n$M)Re(CO)$_3$(α-diimine) (L$_n$M = (CO)$_5$Mn, (CO)$_5$Re, (CO)$_4$Co, Ph$_3$Sn, Cp(CO)$_2$-Fe, etc.) [4,12–26], [M(R)(CO)$_3$(α-diimine)] (M = Mn, Re) [27–31], [(L$_n$M)Ru(Me)(CO)$_2$(α-diimine)] (L$_n$M = (CO)$_5$Mn, (CO)$_5$Re, (CO)$_4$Co) [32,33], [Ru(SnPh$_3$)$_2$-(CO)$_2$(α-diimine) [33,34], and [Ru(I)(*i*Pr)(CO)$_2$(*i*Pr-DAB)] [35] have been studied. Many of these complexes show a homolytic splitting of the metal–metal or metal–alkyl bond on irradiation with visible light. Similar photoreactions occur for the metal–alkyl complexes [Ir(R)(CO)(PAr$_3$)$_2$-(mnt)] [36], [Pt(Me)$_4$(α diimine)] [37], and [Zn(R)$_2$-(α-diimine)] [38], and even for the metal–halide complexes *mer*-[Mn(X)(CO)$_3$(α-diimine)] [39,40].

These light-induced homolysis reactions are assumed to occur from a reactive $^3\sigma\pi^*$ state in which σ represents the high-lying σ-bonding orbital, and π^* the lowest unoccupied orbital of the α-diimine ligand. Recently, several $^3\sigma\pi^*$ states have been detected and characterised with time-resolved absorption, emission and IR spectroscopy [27,34], while alkyl radicals released from Re– and Ru–alkyl complexes

* Corresponding author.

1010-6030/98/$ - see front matter
PII S1010-6030(98)00291-3

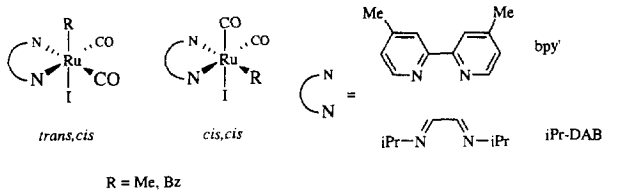

Fig. 1. Schematic molecular structures of the complexes *trans,cis-* and *cis,cis-*[Ru(I)(R)(CO)$_2$(α-diimine)] and of the α-diimine ligands used.

were identified with nanosecond time-resolved FT-EPR spectroscopy [31].

In contrast with the metal–metal bonded complexes the efficiency of the homolytic cleavage of the metal–alkyl bond strongly depends on the alkyl ligand. For instance, the complexes [Re(R)(CO)$_3$(*i*Pr-DAB)] photodecompose into radicals with nearly unit efficiency if R = Bz and Et, but the quantum yield is only 0.05 for R = Me [27]. Similarly, the complexes [Ru(X)(*i*Pr)(CO)$_2$(α-diimine)] [35] photodecompose into radicals with a high quantum yield, whereas [Ru(X)(R)(CO)$_2$(α-diimine)] (R = Me, Et; α-diimine = R-DAB or R-PyCa) are photostable [35]. From these observations it was concluded that only for special alkyl ligands the reactive $^3\sigma\pi^*$ state is close enough in energy to the optically accessible MLCT states that a homolysis reaction can occur. On the other hand, a preliminary study showed that the complex *trans,cis-*[Ru(I)(Me)(CO)$_2$(bpy')] (bpy' = 4,4'-dimethyl-2,2'-bipyridine) is yet photoreactive. This observation prompted us to investigate in more detail the photochemistry of both *trans,cis-* and *cis,cis-*[Ru(I)(Me)-(CO)$_2$(bpy')] and of the corresponding benzyl complexes *trans,cis-*[Ru(I)(Bz)(CO)$_2$(α-diimine)] (α-diimine = bpy', *N,N'*-di-isopropyl-1,4-diazabutadiene (*i*Pr-DAB)). The structures of these complexes and of the α-diimine ligands used are schematically depicted in Fig. 1.

2. Experimental

2.1. Syntheses

The syntheses of the complexes *cis,cis-* and *trans,cis-*[Ru(I)(Me)(CO)$_2$(bpy')] have been described elsewhere [41]. The complexes were identified by FT-IR, UV/Visible, ^{1}H and ^{13}C NMR spectroscopy.

The complexes *trans,cis-*[Ru(I)(Bz)(CO)$_2$(α-diimine)] (α-diimine = *i*Pr-DAB, bpy') were prepared by the procedure described in the literature [41,42]. One equivalent of AgOTf was added to a solution of *trans,cis-*[Ru(X)(Bz)(CO)$_2$(α-diimine)] (X = Cl or Br) in CH_2Cl_2, which was then stirred for 2 h. The residue, AgX, was filtered off and 1 g (excess) (nBu)$_4$NI was added to the solution while light was excluded to prevent photodecomposition. This solution was stirred for 3 h. The excess of (nBu)$_4$NI and (nBu)$_4$NOTf was filtered off and the solvent was evaporated. The complexes were purified by column chromatography on silica using gradient elution with CH_2Cl_2/THF. Yield 50%.

2.1.1. *trans,cis-[Ru(I)(Bz)(CO)$_2$(bpy')]*

^{1}H NMR ($CDCl_3$, 293 K) δ: 8.56 (2H, d, 5.7 Hz, py-H$_6$), 7.89 (2H, s, py-H$_3$), 7.17 (2H, d, 5.7 Hz, py-H$_5$), 6.78 (2H, pst, arom. H), 6.71 (1H, t, 7.1 Hz, arom. H) 6.44 (2H, d, 7.4 Hz, arom. H), 2.52 (2H, s, CH_2–Ph), 2.51 (6H, s, py-CH_3) ppm; ^{13}C NMR ATP ($CDCl_3$, 293 K) δ: 201.6 (Ru–CO), 153.5 (py-C$_2$), 151.7 (py-C$_6$), 150.3 (Ph–C), 149.9 (py-C$_4$), 127.5 (Ph–C), 127.1 (py-C$_3$), 126.3 (Ph–C), 123.1 (Ph–C), 122.1 (py-C$_5$), 20.6 (py-CH_3), 21.2 (CH_2) ppm; IR ν(CO) (CH_2Cl_2, 293 K): 2026 (s); 1961 (s) cm^{-1}; UV/Visible λ (ε in M^{-1} cm^{-1}) (toluene): 415 (1.5×10^3) nm.

2.1.2. *trans,cis-[Ru(I)(Bz)(CO)$_2$(iPr-DAB)]*

^{1}H NMR ($CDCl_3$, 293 K) δ: 8.18 (2H, s, H$_{im}$) 7.10 (2H, pst, arom. H), 6.98 (1H, t, 7.1 Hz, arom. H), 6.90 (2H, d, 7.4 Hz, arom. H), 4.27 (2H, sept, 6.4 Hz, C*H*(CH$_3$)$_2$), 2.30 (2H, s, CH_2–Ph) 1.61/1.41 (3H, d, 6.4 Hz C*H*(CH$_3$)$_2$) ppm; ^{13}C NMR ATP ($CDCl_3$, 293 K) δ: 201.0 (Ru–CO), 157.6 (C$_{im}$), 150.4 (Ph–C), 127.9 (Ph–C), 126.7 (Ph–C), 123.1 (Ph-C), 64.1 (*C*(CH$_3$)$_2$), 25.0/23.0 (C(*C*H$_3$)$_2$) 19.5 (CH_2) ppm; IR ν(CO) (CH_2Cl_2, 293 K): 2033 (s); 1973 (s) cm^{-1}; UV/Visible λ (ε in M^{-1} cm^{-1}) (toluene): 488 (1.6×10^3) nm.

2.2. Materials and equipment

Solvents for spectroscopic measurements and photochemical experiments were of analytical grade, dried over sodium (THF, 2-MeTHF, toluene) or CaH_2 (CH_2Cl_2) and distilled under a N_2 atmosphere. Preparations of the samples were carried out under N_2 by the use of Schlenk techniques. The solutions were carefully handled in the dark before the experiments were performed.

Electronic absorption spectra were measured on a Varian Cary 4E spectrophotometer, infrared spectra on a FTS-60A FTIR spectrometer equipped with a liquid-nitrogen-cooled MCT detector. The ^{1}H and ^{13}C NMR spectra were recorded on a Bruker AMX 300 spectrometer (300.13, 75.46 MHz, respectively) at 293 K. The EPR spectra were measured on a Varian E-104A spectrometer.

Nanosecond time-resolved electronic absorption spectra were obtained by irradiating the sample with 7 ns pulses (FWHM) of a Spectra Physics GCR-3 Nd:YAG laser. The desired excitation wavelength was selected by frequency doubling or tripling of the 1064 nm (10 Hz) fundamental (532 or 355 nm), or by using a Quanta-Ray PDL-pulsed dye laser (Spectra Physics) with a suitable dye (Coumarine 440) pumped by the third harmonic frequency of the Nd:YAG laser. Typical energies were 10 mJ/pulse for all excitation wavelengths. The concentration of the solution was such that the absorbance at the excitation wavelength was between 0.5 and 1.0 and the maximum absorbance did not exceed 1.5. An

EG&G FX-504 high power lamp with a PS-302 power supply was used as the probe source. After passing the sample, the probe light was transferred via an optical fiber to a spectrograph (Acton Spectrapro 150 s Imaging Spectrograph) equipped with a 150 g/mm or 600 g/mm grating and a variable slit (1–500 μm) resulting in 6 nm (150 g/mm) or 1.2 nm (600 g/mm) as the maximum resolution. The data collection system consisted further of a Princeton Instruments model ICCD-576EMG/RB detector, and a Princeton Instruments Programmable Pulse Generator Model PG-200. Further an EG&G Princeton Applied Research Digital Delay Generator Model 9650 was used as the pulse programmer, controlling the probe light, the laser and the pulse generator for the CCD detector. The pump and probe beams were focused perpendicularly on the sample. For the photostable compounds a 1 cm fluorescence cuvette was used, for the photolabile complexes a homemade flow cell and a Verder 2040 pump. The flow speed was ca. 40 ml/min affording a fresh sample every 10 ms after excitation.

2.3. Quantum yield measurements

Quantum yields of the photoreactions were determined by studying the disappearance of the parent complexes by the decay of their visible absorption band. The sample was irradiated within the spectrophotometer by one of the laser lines of an SP2025 Argon-ion laser via in optical fiber and a computer-controlled mechanical shutter. Light intensities were measured with a Coherent model 212 power meter, which was calibrated with an Aberchrome 540 and 540 P solution according to literature methods [43,44]. The 1 cm cuvette was kept at a constant temperature and the solution was vigorously stirred during the measurements. The sample concentration was adjusted to keep the maximum absorbance of the visible absorption band between 1.5 and 1.8. The irradiation time intervals were chosen in such a way that the conversion in each irradiation step was less than 5%. The quantum yields are average values of several measurements. Typical incident light intensities at the irradiation wavelength were $8–13\times10^{-9}$ Einsteins s^{-1}. The programme used to calculate the quantum yields corrects for the changes in the light absorption by the parent compound caused both by its depletion and by the inner filter effect of the photoproduct, according to a previously reported procedure [45,46].

3. Results

The spectroscopic (FTIR, UV/Visible, ^{1}H and ^{13}C NMR) properties of the complexes *cis,cis-* and *trans,cis*-[Ru(I)(Me)(CO)$_2$(bpy′)] have been published before [10, 11,41]. The complex *trans,cis*-[Ru(I)(Bz)(CO)$_2$(*i*Pr-DAB)] has at least two absorption bands in the visible region (see Fig. 2), which are both solvatochromic. This implies that they belong to charge transfer transitions. The two bands arise as a consequence of a strong mixing between the metal-

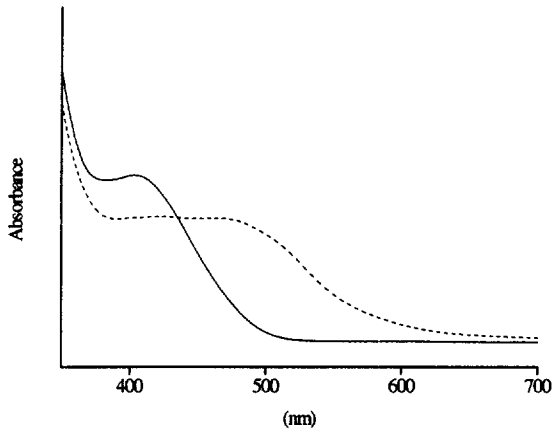

Fig. 2. Electronic absorption spectra of *trans,cis*-[Ru(I)(Bz)(CO)$_2$(α-diimine)] (bpy′ = ———, *i*Pr-DAB = - - -).

d$_\pi$ and halide-p$_\pi$ orbitals. This mixing leads to the formation of two sets of metal–halide orbitals (bonding and antibonding, respectively) and gives rise to two sets of electronic transitions to the lowest π^* orbital of the α-diimine [10,11]. According to the resonance Raman spectra [11] and the DFT MO calculations on the related [Mn(X)(CO)$_3$(bpy)] complexes [49], the lowest-energy (metal–halide antibonding to α-diimine) transitions have more XLCT ($I^- \rightarrow \alpha$-diimine) than MLCT character. Varying the α-diimine ligand from *i*Pr-DAB to bpy′ causes the absorption bands to shift toward shorter wavelengths due to an increase in energy of the lowest π^* orbital of the α-diimine [18,47]. These shifts are in fact so large, that the second absorption band of the bpy′ complex disappears completely under the much stronger absorptions at higher energy. Unless stated otherwise the photoreactions were studied by irradiation into these lowest-energy XLCT transitions of the complexes.

3.1. Continuous wave photolysis

In contrast with the complexes *cis,cis-* and *trans,cis*-[Ru(I)(Me)(CO)$_2$(α-diimine)] (α-diimine = *i*Pr-DAB and *i*Pr-PyCa) [10,48], the complexes *trans,cis*-[Ru(I)(Bz)(CO)$_2$(α-diimine)] (α-diimine = bpy′ and *i*Pr-DAB) and *cis,cis-* and *trans,cis*-[Ru(I)(Me)(CO)$_2$(bpy′)] are very photolabile, even on irradiation into their lowest absorption band ($\lambda > 420$ nm). However, the complexes *trans,cis*-[Ru(I)(Bz)(CO)$_2$(α-diimine)] undergo a completely different photoreaction as *cis,cis-* and *trans,cis*-[Ru(I)(Me)(CO)$_2$(bpy′)]. The IR, UV/Visible and ^{1}H NMR data of the complexes under study and of their photoproducts are collected in Tables 1 and 2.

The in situ irradiation (λ_{exc} = 457.9 nm, RT) of the complex *trans,cis*-[Ru(I)(Me)(CO)$_2$(bpy′)] in CH_2Cl_2 causes a very small change of the ν(CO) bands, from 2030 and 1962 cm^{-1} to 2028 and 1958 cm^{-1}. The same frequency shifts are observed in $CHCl_3$, THF and toluene. More drastic changes occur in the UV/Visible and ^{1}H NMR spectra. The absorption spectrum shows the disappearance of the 397 nm band of the

Table 1
IR ν(CO) frequencies of [Ru(I)(R)(CO)$_2$(α-diimine)] (R = Me, Bz; α-diimine = bpy', *i*Pr-DAB) and their photoproducts in different solvents

Compound	Solvent	ν(CO) cm^{-1}	λ_{max} (nm)
trans,cis-[Ru(I)(Me)(CO)$_2$(bpy')]	DCM	2030 (s) 1962 (s)	405; 363
cis,cis-[Ru(I)(Me)(CO)$_2$(bpy')]	DCM	2025 (s) 1952 (s)	400
trans,cis-[Ru(I)(Bz)(CO)$_2$(bpy')]	Toluene	2024 (s) 1960 (s)	
trans,cis-[Ru(I)(Bz)(CO)$_2$(*i*Pr-DAB)]	Toluene	2030 (s) 1971 (s)	488
trans,cis-[Ru(I)$_2$(CO)$_2$(bpy')]	Toluene	2051 (s) 1994 (s)	
trans,cis-[Ru(I)$_2$(CO)$_2$(*i*Pr-DAB)]	Toluene	2054 (s) 2002 (s)	
[Ru(Bz)(CO)$_2$(*i*Pr-DAB)]$_2$	Toluene	1961 (s) 1935 (m)[a]	750
[Ru(I)(Me)(CO)(DMSO)(bpy')]	DMSO	1933 (s)	430 (sh)

[a]High frequency band obscured by parent or product band.

Table 2
^{1}H NMR data of [Ru(I)(Me)(CO)$_2$(bpy')] and the photoproducts in different solvents

Compound	^{1}H NMR (ppm)
trans,cis-[Ru(I)(Me)(CO)$_2$(bpy')][a]	8.79 (2H, d, 6 Hz, py-H$_6$), 8.00 (2H, s, py-H$_3$), 7.34 (2H, d, 6 Hz, py-H$_5$), 2.56 (6H, s, py-Me), 0.11 (3H, s, Ru-Me)
cis,cis-[Ru(I)(Me)(CO)$_2$(bpy')][a]	8.81/8.80 (1H, d, 6 Hz, py-H$_{6/6'}$), 8.04/8.00 (1H, s, py-H$_{3/3'}$), 7.41/7.31 (1H, d, 6 Hz, py-H5/5'), 2.58/2.55 (3H, s, py-Me/py-Me'), 0.80 (3H, s, Ru-Me)
trans,cis-[Ru(I)(Me)(CO)2(bpy')][b]	8.79 (2H, d, 6 Hz, py-H$_6$), 8.58 (2H, s, py-H$_3$), 7.55 (2H, d, 6 Hz, py-H$_5$), 0.04 (3H, s, Ru-Me)
cis,cis-[Ru(I)(Me)(CO)$_2$(bpy')][b]	8.84/8.73 (1H, d, 6 Hz, py-H$_{6/6'}$), 8.60/8.56 (1H, s, py-H$_{3/3'}$), 7.64/7.52 (1H, d, 6 Hz, py-H$_{5/5'}$), 0.70 (3H, s, Ru-Me)
[Ru(I)(Me)(CO)(DMSO)(bpy')][b]	8.87/8.69 (1H, d, 6 Hz, py-H$_{6/6'}$), 8.53/8.49 (1H,s, py-H$_{3/3'}$), 7.59/7.45 (1H, d, 6 Hz, py-H$_{5/5'}$), 0.46 (3H, s, Ru-Me)

[a]In d^2-DCM.
[b]In d^6-DMSO.

parent compound and the formation of a product having absorption maxima at approximately 400 and 360 nm.

In order to identify the photoproduct, the photolysis of *trans,cis*-[Ru(I)(Me)(CO)$_2$(bpy')] was followed in situ with ^{1}H NMR, using a special CIDNP probe in which the sample was irradiated ($\lambda_{exc} > 420$ nm) within the NMR magnet. Fig. 3 shows the ^{1}H NMR spectra measured at different intervals of irradiation in d^2-DCM at RT. The proton signals of the starting compound (bottom spectrum in Fig. 3) convert

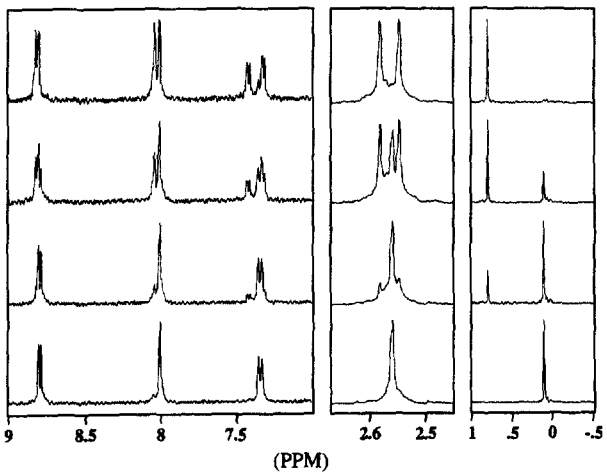

Fig. 3. ^{1}H NMR spectral changes accompanying the photoreaction of *trans,cis*-[Ru(I)(Me)(CO)$_2$(bpy')] (bottom) to give *cis,cis*-[Ru(I)-(Me)(CO)$_2$(α-diimine)] (top) (in d^2-DCM, $\lambda_{exc} > 420$).

smoothly and quantitatively into those of the photoproduct (top spectrum). The complexed bpy' ligand shows two sets of signals for the protons in the region 9–6 ppm and in the region 2.7–2.3 ppm, while the proton signals of the methyl ligand shift to a higher ppm value (0.11 → 0.80 ppm). The proton resonances and the splitting constants are identical to those of *cis,cis*-[Ru(I)(Me)(CO)$_2$(bpy')], an isomer of the starting complex in which the methyl ligand has moved from an axial to an equatorial position [41]. The IR and UV/Visible spectra of the photoproduct are also identical to those of this *cis,cis*-isomer [41].

In order to elucidate the mechanism of this photoisomerisation reaction, the photolysis was carried out in strongly coordinating solvents and also in the presence of various nucleophiles. Photolysis of both *trans,cis*- and *cis,cis*-[Ru(I)(Me)(CO)$_2$(bpy')] in d^6-DMSO gave rise to a relatively clean reaction producing a single, thermally stable, product. The spectroscopic data of this photoproduct are collected in Tables 1 and 2. Fig. 4 shows the ^{1}H NMR spectra obtained at different stages of the in situ photoreaction ($\lambda_{exc} > 320$ nm) of the *trans,cis*- and *cis,cis*-complexes in d^6-DMSO. The methyl resonances of bpy' are obscured by solvent peaks. The spectra clearly show the formation of the same photoproduct for both the *trans,cis*- and *cis,cis*-isomer. The FTIR spectra reveal the formation of a product with one ν(CO) band at 1933 cm^{-1}, while the UV/Visible absorption band shifts from 380 to 430 nm. Evidently, the primary

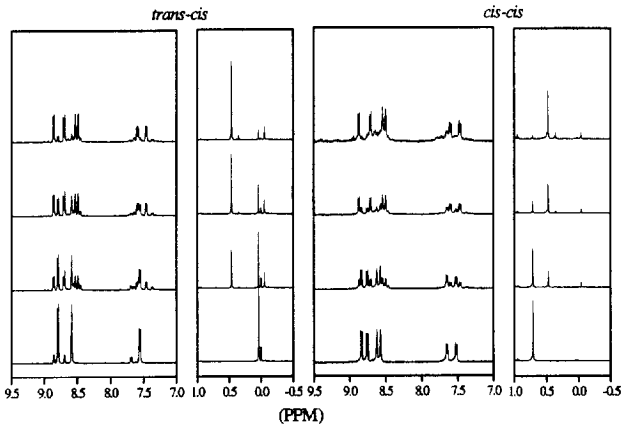

Fig. 4. ^{1}H NMR spectral changes accompanying the photoreaction of *trans,cis* (left, bottom) and *cis,cis*-[Ru(I)(Me)(CO)$_2$(bpy′)] (right, bottom) to give [Ru(I)(Me)(CO)(d^6-DMSO)(α-diimine)] (top) (in d^6-DMSO, $\lambda_{exc} > 320$ nm).

photoprocess is a CO-loss reaction, resulting in a product possessing only one CO ligand. Based on the relatively small splitting of the proton resonances of the bpy′ ligand, which are very similar to those found for the *cis,cis*-complex, this intermediate of the photoisomerisation reaction is proposed to have the structure depicted in Scheme 1.

Photolysis of *trans,cis*-[Ru(I)(Me)(CO)$_2$(bpy′)] in other solvents such as CD_3CN, d^5-pyridine or in d^2-DCM in the presence of an excess (1:10 up to 100) or equimolar quantity of PEt_3, PPh_3 or $POMe_3$, always results in the formation of unidentifiable photoproducts. However, rapid scan FTIR experiments in CH_3CN and in pyridine shows again the formation of a single photoproduct with only one ν(CO) band at approximately 1940 cm^{-1}. This photoproduct decomposes thermally and new ν(CO) bands appear at nearly the same position. The time scale of this thermal follow-up reaction is in the order of seconds. When the photoreaction is instead performed at 253 K, the same photoproduct appears, but even at this temperature its thermal decomposition cannot be avoided. These secondary reactions were not further investigated due to the complexity of the product formation.

Irradiation ($\lambda_{exc} > 420$) of the corresponding benzyl complex *trans,cis*-[Ru(I)(Bz)(CO)$_2$(*i*Pr-DAB)] causes a shift of the ν(CO) bands from 2030 and 1971 cm^{-1} to 2054 and 2002 cm^{-1} and a decrease of their intensities to about half the original values. In addition, two other IR bands are found at 1961 and 1935 cm^{-1}. Prolonged irradiation of the solution results in the formation of various other products, which were not further investigated. The solvent has no influence on the

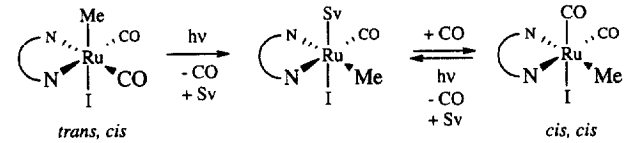

Scheme 1. Proposed mechanism of the photoreactions of *trans,cis*- and *cis,cis*-[Ru(I)(Me)(CO)$_2$(bpy′)].

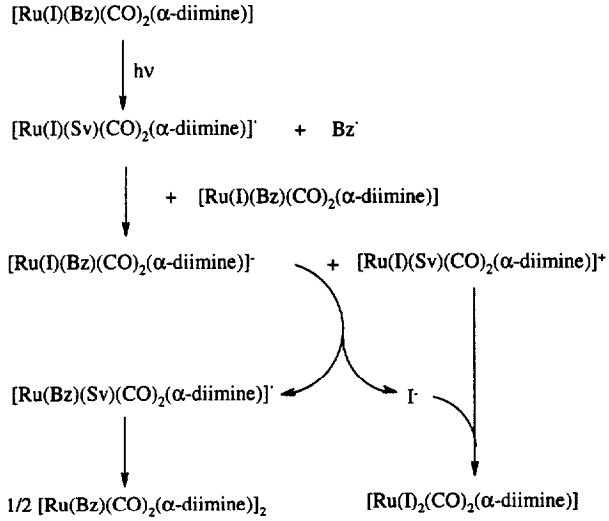

Scheme 2. Proposed mechanism of the photoreaction of *trans,cis*-[Ru(I)(Bz)(CO)$_2$(α-diimine)] (α-diimine = bpy′, *i*Pr-DAB).

course of the photoreaction, since the same photoproduct is formed in CH_2Cl_2, CH_2Cl_2/CCl_4, THF, and toluene. The reaction product is similar to that obtained for the corresponding complex *trans,cis*-[Ru(I)(*i*Pr)(CO)$_2$(*i*Pr-DAB)], viz. *trans,cis*-[Ru(I)$_2$(CO)$_2$(*i*Pr-DAB)] [35]. The formation of this product by irradiation of *trans,cis*-[Ru(I)(Bz)-(CO)$_2$(*i*Pr-DAB)] will therefore proceed by the same mechanism as proposed for the isopropyl analogue [35]. According to this mechanism, depicted in Scheme 2, the primary photoprocess is a homolytic splitting of the Ru–Bz bond.

However, contrary to the photochemical reaction of *trans,cis*-[Ru(I)(*i*Pr)(CO)$_2$(*i*Pr-DAB)] [35], the corresponding benzyl complex gives rise to the formation of a second photoproduct having ν(CO) bands at 1961 and 1935 cm^{-1} and an absorption band at ca. 750 nm. Such a band between 700 and 800 nm has been observed before for several metal–metal bonded dimers containing two chelating α-diimine ligands [16,17,49,50]. For instance, the related dimer [Ru(Me)(CO)$_2$(*i*Pr-DAB)]$_2$ has ν(CO) bands at 1982, 1955 and 1925 cm^{-1} and a strong absorption band at 750 nm [50]. The band at ca. 1982 cm^{-1} is not observed during the reaction of *trans,cis*-[Ru(I)(Bz)(CO)$_2$(*i*Pr-DAB)]; it is most likely obscured by IR bands of the parent complex or of the *trans,cis*-[Ru(I)$_2$(CO)$_2$(*i*Pr-DAB)] product. Similarly, irradiation ($\lambda_{exc} = 457.9$ nm) of the corresponding bpy′-complex *trans,cis*-[Ru(I)(Bz)(CO)$_2$-(bpy′)] results in the formation of *trans,cis*-[Ru(I)$_2$(CO)$_2$-(bpy′)] without, however, any evidence of dimer formation.

3.2. EPR spectra

Irradiation ($\lambda_{exc} > 420$ nm) at room temperature of a toluene solution of *trans,cis*-[Ru(I)(Bz)(CO)$_2$(α-diimine)] (α-diimine = bpy′, *i*Pr-DAB) with an excess of nitrosodurene (1:5) affords an EPR spectrum of the radical (CH$_3$)$_4$-(C$_6$H)N(O·)–CH$_2$(C$_6$H$_5$). The spectrum shows nine lines due to the coupling of the unpaired electron with the nitrogen

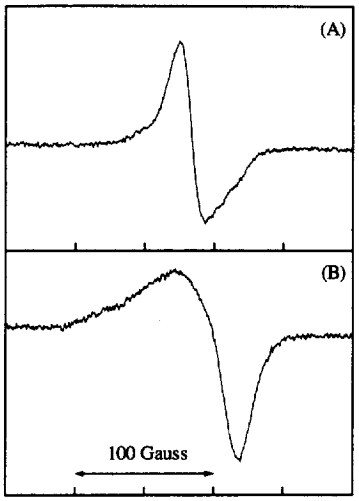

Fig. 5. EPR spectra measured after irradiation of *trans,cis*-[Ru(I)(Bz)-$(CO)_2$(α-diimine)] in 2-MeTHF at 133 K (A) α-diimine = bpy′ (B) α-diimine = *i*Pr-DAB.

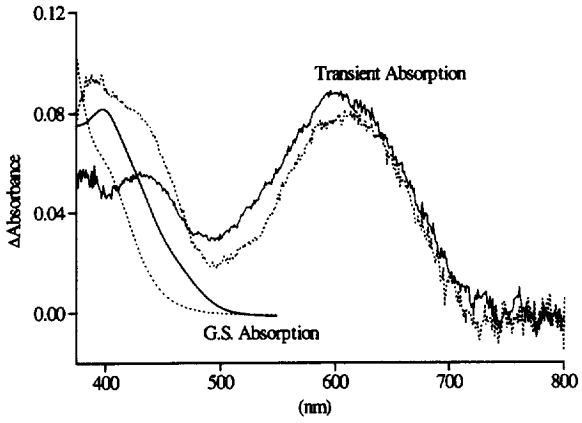

Fig. 6. Ground state absorption and transient absorption spectra of [Ru(I)(Me)$(CO)_2$(bpy′)] (*trans,cis* = ———, *cis,cis* = - - -) measured 10 ns after the pulse (THF, λ_{exc} = 355 nm).

nucleus ($I_N = 1$) and the two hydrogen nuclei ($I_H = 1/2$) of the benzyl group. The coupling constants, $a_N = 13.8$ G and $a_H = 8.0$ G, obtained by simulation of the spectrum, are in excellent agreement with literature data [27,35,51]. As the EPR spectra do not show any signal of a metal radical-fragment, the two benzyl complexes were also irradiated ($\lambda_{exc} > 420$ nm) in a 2-MeTHF glass at 133 K.

The resulting EPR spectra (Fig. 5) are broad and anisotropic, the average g-value is estimated at $g \approx 2.008$. From these spectra no information could be obtained about the hyperfine splitting constants, although different line shapes are observed when the bpy′ ligand is replaced by *i*Pr-DAB. These radical signals are therefore tentatively assigned to [Ru(I)(2-MeTHF)$(CO)_2$(*i*Pr-DAB)]$^{\bullet}$ and [Ru(I)(2-MeTHF)$(CO)_2$(bpy′)]$^{\bullet}$, respectively.

3.3. Quantum yields

The efficiency of the homolysis reaction of *trans,cis*-[Ru(I)(Bz)$(CO)_2$(*i*Pr-DAB)] and of the photoisomerisation of *trans,cis*-[Ru(I)(Me)$(CO)_2$(bpy′)] was determined by measuring the quantum yield (Φ) for the disappearance of the parent compounds at various temperatures and in the case of *trans,cis*-[Ru(I)(Bz)$(CO)_2$(*i*Pr-DAB)] also at various wavelengths. The results are summarised in Table 3. The quantum yield of the homolysis reaction of *trans,cis*-[Ru(I)(Bz)$(CO)_2$(*i*Pr-DAB)] is nearly temperature independent. Attempts to measure the quantum yield for the corresponding *trans,cis*-[Ru(I)-(Bz)$(CO)_2$(bpy′)] complex failed due to the strong absorption and photolability of the photoproduct *trans,cis*-[$Ru(I)_2(CO)_2$(bpy′)].

The quantum yield of the photoisomerisation of *trans,cis*-[Ru(I)(Me)$(CO)_2$(bpy′)] into *cis,cis*-[Ru(I)(Me)-$(CO)_2$(bpy′)] strongly depends on the temperature. This temperature effect corresponds to an activation energy of 42.8 kJ mol^{-1} or 3530 cm^{-1} as calculated from the Arrhenius equation ($k = A \cdot e^{-E_a/RT}$).

3.4. Transient absorption spectra

Nanosecond flash photolysis experiments were carried out for all complexes in THF and toluene using 355 or 532 nm laser pulse excitation. Fig. 6 shows the ground state and transient spectra of *cis,cis*- and *trans,cis*-[Ru(I)(Me)-$(CO)_2$(bpy′)] in THF at room temperature.

The transient spectra were measured 5 ns after the laser pulse. For both the *cis,cis* and *trans,cis* complex identical transients are observed in the region 500 to 800 nm. The difference in the region 375–500 nm is ascribed to a different

Table 3
Quantum yields of the photoreactions of *trans,cis*-[Ru(I)(Me)$(CO)_2$(bpy′)] and *trans,cis*-[Ru(I)(Bz)$(CO)_2$(*i*Pr-DAB)]

[Ru(I)(Me)$(CO)_2$(bpy′)][a]		[Ru(I)(Bz)$(CO)_2$(*i*Pr-DAB)][b]			
T (K)	457.9 nm	T (K)	457.9 nm	488.0 nm	514.5 nm
298	0.98 ± 0.01	293	1.08 ± 0.02	1.03 ± 0.04	1.07 ± 0.07
293	0.75 ± 0.01	273	1.01 ± 0.03	0.85 ± 0.02	0.81 ± 0.04
288	0.59 ± 0.03	253	0.88 ± 0.01	0.82 ± 0.02	0.66 ± 0.08
283	0.41 ± 0.02				
278	0.28 ± 0.04				

[a]In DCM.
[b]In toluene.

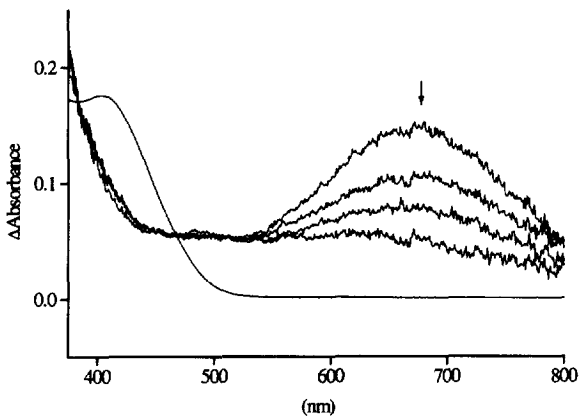

Fig. 7. Ground state absorption and transient absorption spectra of *trans,cis*-[Ru(I)(Bz)(CO)$_2$(bpy′)] measured 10 ns, 1, 2 and 5 μs after the pulse (toluene, λ_{exc} = 355 nm).

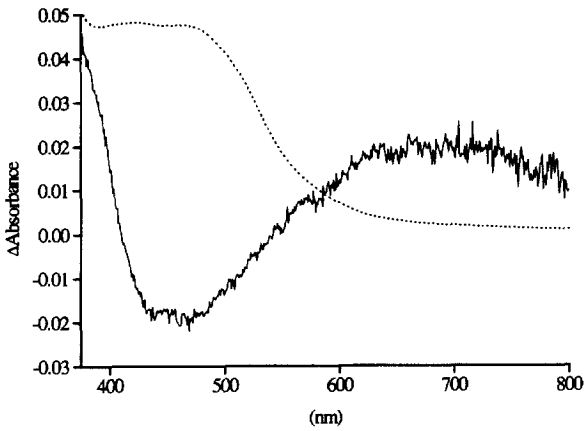

Fig. 8. Ground state absorption (- - -) and transient (———) absorption spectrum of *trans,cis*-[Ru(I)(Bz)(CO)$_2$(*i*Pr-DAB)] measured 10 ns after the pulse (toluene, λ_{exc} = 355 nm).

bleach of the parent complex. When the right correction is applied for the bleach, identical spectra are indeed obtained. The transient absorptions last for at least 10 μs, and the same spectra are obtained in THF and toluene.

Figs. 7 and 8 show the ground state and transient absorption spectra of *trans,cis*-[Ru(I)(Bz)(CO)$_2$(bpy′)] and *trans,cis*-[Ru(I)(Bz)(CO)$_2$(*i*Pr-DAB)], respectively. The spectra of *trans,cis*-[Ru(I)(Bz)(CO)$_2$(bpy′)], measured within the time domain 10 ns–5 μs, exhibit a strong transient absorption, which is dominated by a band at ca. 690 nm in THF and 720 nm in toluene. The decay of the transient is multiexponential and comparable in both solvents. The complex *trans,cis*-[Ru(I)(Bz)(CO)$_2$(*i*Pr-DAB)] shows a transient with a broad maximum at 680 nm and a strong absorption at approximately 350 nm, which does not depend on the solvent (THF/toluene). This transient does not change during at least 10 μs.

4. Discussion

Irradiation of *trans,cis*-[Ru(I)(Me)(CO)$_2$(bpy′)] causes the formation of its *cis,cis*-isomer. This photoisomerisation is, however, not a primary photoprocess as evidenced by the reaction in DMSO and by the nanosecond transient absorption spectra. In DMSO and other coordinating solvents, the photoisomerisation does not occur. Instead a CO ligand is released with formation of the same photosubstitution product for *cis,cis* and *trans,cis*-[Ru(I)(Me)(CO)$_2$(bpy′)]. According to the transient absorption spectra in toluene and THF, this CO-loss product is the primary photoproduct as well as the intermediate of the photoisomerisation reaction taking place in these solvents. For, the transient spectra show the presence within the laser pulse of the same transient species for both isomers absorbing at approximately 600 nm. Such a shift to longer wavelength normally accompanies the replacement of an electron withdrawing carbonyl ligand by an electron releasing solvent molecule; it has also been observed for the CO-loss products of the related complexes [Mn(Me)(CO)$_3$(*i*Pr-DAB)] [28], and [Mn(Br)(CO)$_3$(*i*Pr-DAB)] [39]. With the CO-loss products as intermediates, the photoisomerisation reaction will proceed according to Scheme 1. In this scheme it has been taken into account that irradiation of both isomers affords the same CO-loss product. According to this scheme excitation of *trans,cis*-[Ru(I)(Me)(CO)$_2$(bpy′)] gives rise to release of CO, a shift of the methyl ligand to an equatorial position, and occupation of the open axial site by a solvent molecule. The same mechanism has been proposed for the above mentioned Mn complexes and has been derived theoretically for the photoisomerisation of the model complex *fac*-[Mn(Cl)(CO)$_3$(H-DAB)] [52]. The position of the charge transfer band of the CO-loss product will depend on the solvent used. For DMSO it does not deviate much from that of the *cis,cis*-[Ru(I)(Me)(CO)$_2$(bpy′)] complex, in THF and CH_2Cl_2 it is at much lower energy because of the weakly or noncoordinating properties of the solvent molecules. As shown in Table 3 the quantum yield of the *trans,cis* → *cis,cis* photoisomerisation strongly depends on the temperature. The activation energy of 3530 cm^{-1} will not be due to the CO-loss reaction but to the shift of the methyl ligand from the axial to the equatorial position. This is evident from the observation that both the *trans,cis* and *cis,cis* isomer show an efficient CO loss reaction even at 253 K, the *cis,cis* isomer being even photolabile in a 2-MeTHF glass at 80 K.

The transient absorption spectra of *trans,cis*-[Ru(I)(Bz)(CO)$_2$(α-diimine)] (α-diimine = bpy′, *i*Pr-DAB) are very similar to the absorptions of the radical species [Ru(I)(Sv)(CO)$_2$(α-diimine)]$^{\bullet}$ (Sv = Solvent). Thus, the transient species formed by excitation of *trans,cis*-[Ru(I)(Bz)(CO)$_2$(*i*Pr-DAB)] shows a strong absorption at ca. 350 nm, which has also been observed in the transient spectra of *trans,cis*-[Ru(I)(*i*Pr)(CO)$_2$(*i*Pr-DAB)] [35] and for the radical species [Ru(Me)(PPh_3)(CO)$_2$(*i*Pr-DAB)]$^{\bullet}$ [53] and [Re(CO)$_3$(*i*Pr-DAB)]$^{\bullet}$ [54]. This 350 nm band is accordingly assigned to the radical [Ru(I)(Sv)(CO)$_2$(*i*Pr-DAB)]$^{\bullet}$. The transient absorption spectrum obtained by irradiation of the corresponding bpy′ complex *trans,cis*-[Ru(I)(Bz)(CO)$_2$(bpy′)] has its main absorption band at

ca. 700 nm. This band is again assigned to the radical species $[Ru(I)(Sv)(CO)_2(bpy')]^{\bullet}$, because of its close resemblance with that of the electrochemically generated radical $[Ru(Me)(prCN)(CO)_2(bpy)]^{\bullet}$ (λ_{max} = 640 nm) [53]. According to these observations the complexes *trans,cis*-$[Ru(I)(Bz)(CO)_2(\alpha\text{-diimine})]$ photodecompose into radicals by homolysis of the metal–benzyl bond and this reaction is completed within less than 10 ns. This result is in agreement with the time-resolved FT-EPR spectra of the complexes *trans,cis*-$[Ru(I)(R)(CO)_2(i\text{Pr-DAB})]$ (R = *i*Pr, Bz) which reveal the presence of alkyl radicals on a nanosecond time scale [31]. Although the benzyl and $[Ru(I)(Sv)(CO)_2(\alpha\text{-diimine})]^{\bullet}$ (α-diimine = bpy', *i*Pr-DAB) radicals were not stable enough to be detected with CW-EPR at room temperature, the benzyl radicals could be observed with the use of a spin-trap, and the $[Ru(I)(Sv)(CO)_2(\alpha\text{-diimine})]^{\bullet}$ radicals were stable enough at low temperature to give rise to an EPR signal. This again demonstrates the occurrence of a homolysis reaction.

After homolysis of the Ru–Bz bond, the coordinately unsaturated $[Ru(I)(CO)_2(\alpha\text{-diimine})]^{\bullet}$ radical reacts as depicted in Scheme 2. The radical takes up a solvent molecule (Sv) and then reduces the parent complex, with the formation of $[Ru(I)(Sv)(CO)_2(\alpha\text{-diimine})]^{+}$ and $[Ru(I)(Bz)(CO)_2(\alpha\text{-diimine})]^{-}$. The multiexponential decay, observed for the transient absorption spectra of *trans,cis*-$[Ru(I)(Bz)(CO)_2(bpy')]$, points to an electron transfer chain (ETC) mechanism for this reaction. Similar ETC mechanisms have been proposed for the photoreactions of *trans,cis*-$[Ru(I)(i\text{Pr})(CO)_2(\alpha\text{-diimine})]$ [35] and $[CO_5Mn(CO)_3(\alpha\text{-diimine})]$ [55].

The anions $[Ru(I)(Bz)(CO)_2(\alpha\text{-diimine})]^{-}$ lose I^{-}, and produce the radicals $[Ru(Sv)(Bz)(CO)_2(\alpha\text{-diimine})]^{\bullet}$, which dimerise to give $[Ru(Bz)(CO)_2(\alpha\text{-diimine})]_2$. This reaction process agrees with the observation that the reduction of the complexes $[Ru(X)(R)(CO)_2(\alpha\text{-diimine})]$ results in loss of X^{-} and in the formation of the dimeric compound $[Ru(R)(CO)_2(\alpha\text{-diimine})]_2$ [50]. The stability of these dimers $[Ru(R)(CO)_2(\alpha\text{-diimine})]_2$ strongly depends on the alkyl and α-diimine ligand. In fact, they are not stable if these ligands are too electron releasing. Thus, the dimer is not formed in the case of *trans,cis*-$[Ru(I)(i\text{Pr})(CO)_2(i\text{Pr-DAB})]$ and also not for the bpy' complexes.

The iodide, released from the unstable anion $[Ru(I)(Bz)(CO)_2(\alpha\text{-diimine})]^{-}$ reacts with the cation $[Ru(I)(Sv)(CO)_2(\alpha\text{-diimine})]^{+}$ with formation of *trans,cis*-$[Ru(I)_2(CO)_2(\alpha\text{-diimine})]$. According to Scheme 2 the formation of one radical results in the disappearance of two parent molecules. This implies that the disappearance quantum yields collected in Table 3 are twice as high as those of the primary photoprocess.

4.1. Homolysis vs. CO-loss

Radical formation after excitation into the lowest-energy absorption band, as observed for *trans,cis*-$[Ru(I)(Bz)(CO)_2(\alpha\text{-diimine})]$ (α-diimine = *i*Pr-DAB and bpy') has also been established for *trans,cis*-$[Ru(I)(i\text{Pr})(CO)_2(i\text{Pr-DAB})]$ [35] and for related metal–metal bonded and metal–alkyl complexes [4,12–34]. For the complexes $[Zn(R)_2(R\text{-DAB})]$ the homolysis reaction proceeds from the $^3\sigma\pi^*$ state by direct irradiation into the $\sigma(Zn\text{-}R) \rightarrow \pi^*(R\text{-DAB})$ transition [38]. The metal-d orbitals are too low in energy to be involved in this process. The situation is, however, quite different for the transition-metal (Mn, Re, Ru, Os) complexes showing a similar homolysis reaction, since the metal-d orbitals are close in energy to the σ orbital and strongly mix with the π^* orbital of the α-diimine (π-backbonding). Because of this mixing, the $d_\pi \rightarrow \pi^*$ (MLCT) transition (or the $p_\pi(X) \rightarrow \pi^*$ transition in the case of the halide complexes under study) is normally the main low-energy transition and the $\sigma \rightarrow \pi^*$ transition is overlap forbidden. The homolysis reaction is then proposed to occur by MLCT or XLCT excitation followed by a surface crossing to the reactive $^3\sigma\pi^*$ state. The involvement of a reactive triplet state, viz. $^3\sigma\pi^*$, was evidenced by the results of a time-resolved FT-EPR study on the complexes $[Re(R)(CO)(bpy')]$ (R = Et, *i*Pr, Bz), *trans,cis*-$[Ru(I)(i\text{Pr})(CO)_2(i\text{Pr-DAB})]$ and *trans,cis*-$[Ru(I)(Bz)(CO)_2(i\text{Pr-DAB})]$ [31]. According to this mechanism the efficiency of the homolysis reaction will depend not only on the reactivity of the $^3\sigma\pi^*$ state, but also on the relative energies of the optically accessible, nonreactive MLCT/XLCT states and reactive $^3\sigma\pi^*$ state. Thus, for the complexes $[Re(R)(CO)_3(i\text{Pr-DAB})]$ the quantum yield of the homolytic splitting of the Re–R bond depends on R. When R = Me the quantum yield is only 0.05, while for R = Et, Bz the reaction proceeds with nearly unit efficiency [27]. Such high quantum yields are also observed for the homolysis of the Ru–Bz bond in the case of *trans,cis*-$[Ru(I)(Bz)(CO)_2(i\text{Pr-DAB})]$ (see Table 3) and of the Ru–*i*Pr bond in the corresponding *i*Pr-complex [35]. This implies that the $^3\sigma\pi^*$ state is lower in energy than the optically accessible XLCT states (see Fig. 9). However, in contrast to the Re-compounds, the photoreactivity of the Ru-complexes does not merely vary with R, the photoreaction itself changes just as in the case of the $[Mn(R)(CO)_3(\alpha\text{-diimine})]$ complexes [28]. Thus, the *cis,cis*- and *trans,cis*-$[Ru(I)(Me)(CO)_2(bpy')]$ complexes do not show a homolysis reaction as the benzyl and isopropyl compounds, but lose CO on XLCT excitation. This implies that the XLCT

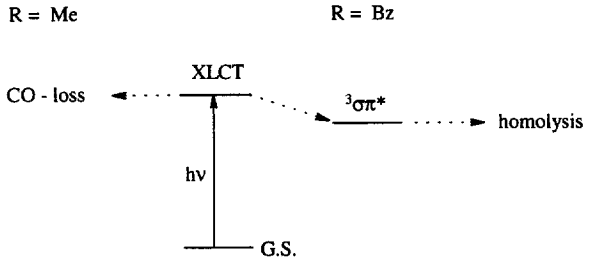

Fig. 9. Schematic energy level diagram of *trans,cis*-$[Ru(I)(R)(CO)_2(bpy')]$ (R = Me, Bz).

state itself is reactive or that it crosses a reactive, e.g., LF state from which the CO-loss reaction occurs. As XLCT and MLCT states are normally not reactive, the latter explanation is preferred, the more since this reaction is only observed for the bpy′ complexes, which have their XLCT states higher in energy, i.e., closer to the reactive LF states. Similar reactions were observed for the complexes $[Mn(Me)(CO)_3(i$Pr-DAB)] [28], $[Mn(Br)(CO)_3(\alpha$-diimine)] [39] and $[Cr(CO)_4(\alpha$-diimine)] [45], for which population of an MLCT state also leads to CO dissociation (see Fig. 9). Normally the quantum yield of such a reaction is rather low, but for *trans,cis*-$[Ru(I)(Me)(CO)_2(bpy')]$ the reaction proceeds with nearly unit efficiency at room temperature.

5. Conclusion

Variation of the alkyl or α-diimine ligand in *trans,cis*-$[Ru(X)(R)(CO)_2(\alpha$-diimine)] not only influences its photoreactivity, but may also change the type of reaction taking place. Even more, since X and R can nearly be replaced at will, these Ru-complexes are very well suited to tune their excited state properties.

Acknowledgements

Prof. A. Oskam is thanked for stimulating discussions and critical reading of the manuscript. Thanks are due to the Netherlands Foundation for Chemical Research (SON) and the Netherlands Organisation for the Advancement of Pure Research (NWO) for financial support.

References

[1] K. Kalyanasundaram, Coord. Chem. Rev. 46 (1982) 159.
[2] R.J. Watts, J. Chem. Educ. 60 (1983) 834.
[3] H. Riesen, Y. Gao, E. Krausz, Chem. Phys. Lett. 228 (1994) 610.
[4] D.J. Stufkens, Comments Inorg. Chem. 13 (1992) 359.
[5] T.A. Perkins, W. Humer, T.L. Netzel, K.S. Schanze, J. Phys. Chem. 94 (1990) 2229.
[6] P. Chen, T.D. Westmoreland, E. Danielson, K.S. Schanze, D. Anthon, P.E. Neveux Jr., T.J. Meyer, Inorg. Chem. 26 (1987) 1116.
[7] K.S. Schanze, D.B. MacQueen, T.A. Perkins, L.A. Cabana, Coord. Chem. Rev. 122 (1993) 63.
[8] L.A. Worl, R. Duesing, P. Chen, L.D. Ciana, T.J. Meyer, J. Chem. Soc., Dalton Trans. (1991) 849.
[9] B.D. Rossenaar, D.J. Stufkens, A. Vlček Jr., Inorg. Chem. 35 (1996) 2902.
[10] H.A. Nieuwenhuis, D.J. Stufkens, A. Vlček Jr., Inorg. Chem. 34 (1995) 3879.
[11] H.A. Nieuwenhuis, D.J. Stufkens, A. Oskam, Inorg. Chem. 33 (1994) 3212.
[12] J.C. Luong, R.A. Faltynek, M.S. Wrighton, J. Am. Chem. Soc. 102 (1980) 7892.
[13] J.C. Luong, R.A. Faltynek, M.S. Wrighton, J. Am. Chem. Soc. 101 (1979) 1597.
[14] D.L. Morse, M.S. Wrighton, J. Am. Chem. Soc. 98 (1976) 3931.
[15] M.W. Kokkes, D.J. Stufkens, A. Oskam, Inorg. Chem. 24 (1985) 2934.
[16] M.W. Kokkes, W.G.J. De Lange, D.J. Stufkens, A. Oskam, J. Organomet. Chem. 294 (1985) 59.
[17] M.W. Kokkes, D.J. Stufkens, A. Oskam, Inorg. Chem. 24 (1985) 4411.
[18] D.J. Stufkens, Coord. Chem. Rev. 104 (1990) 39.
[19] R.R. Andréa, W.G.J. de Lange, D.J. Stufkens, A. Oskam, Inorg. Chem. 28 (1989) 318.
[20] H.K. van Dijk, J. van der Haar, D.J. Stufkens, A. Oskam, Inorg. Chem. 28 (1989) 75.
[21] T. van der Graaf, D.J. Stufkens, A. Oskam, K. Goubitz, Inorg. Chem. 30 (1991) 599.
[22] T. van der Graaf, A. van Rooy, D.J. Stufkens, A. Oskam, Inorg. Chim. Acta 187 (1991) 133.
[23] J.W.M. van Outersterp, D.J. Stufkens, A. Vlček Jr., Inorg. Chem. 34 (1995) 5183.
[24] B.D. Rossenaar, T. van der Graaf, R. van Eldik, C.H. Langford, D.J. Stufkens, A. Vlček Jr., Inorg. Chem. 33 (1994) 2865.
[25] B.D. Rossenaar, E. Lindsay, D.J. Stufkens, A. Vlček Jr., Inorg. Chim. Acta 250 (1996) 5.
[26] P.C. Servaas, G.J. Stor, D.J. Stufkens, A. Oskam, Inorg. Chim. Acta 178 (1990) 185.
[27] B.D. Rossenaar, C.J. Kleverlaan, M.C.E. van de Ven, D.J. Stufkens, A. Vlček Jr., Chem. Eur. J. 2 (1996) 228.
[28] B.D. Rossenaar, D.J. Stufkens, A. Oskam, J. Fraanje, K. Goubitz, Inorg. Chim. Acta 247 (1996) 215.
[29] B.D. Rossenaar, C.J. Kleverlaan, M.C.E. van de Ven, D.J. Stufkens, A. Oskam, J. Fraanje, K. Goubitz, J. Organomet. Chem. 493 (1995) 153.
[30] B.D. Rossenaar, M.W. George, F.P.A. Johnson, D.J. Stufkens, J.J. Turner, A. Vlček Jr., J. Am. Chem. Soc. 117 (1995) 11582.
[31] C.J. Kleverlaan, D.M. Martino, H.v. Willigen, D.J. Stufkens, A. Oskam, J. Phys. Chem. 100 (1996) 18607.
[32] H.A. Nieuwenhuis, A. van Loon, M.A. Moraal, D.J. Stufkens, A. Oskam, K. Goubitz, J. Organomet. Chem. 492 (1995) 165.
[33] M.P. Aarnts, D.J. Stufkens, A. Vlček Jr., Inorg. Chim. Acta 266 (1997) 37.
[34] M.P. Aarnts, D.J. Stufkens, M.P. Wilms, E.J. Baerends, A. Vlček Jr., I.P. Clark, M.W. George, J.J. Turner, Chem. Eur. J. 2 (1996) 1556.
[35] H.A. Nieuwenhuis, M.C.E. van de Ven, D.J. Stufkens, A. Oskam, K. Goubitz, Organometallics 14 (1995) 780.
[36] P. Bradley, G. Suardi, A.P. Zipp, R. Eisenberg, J. Am. Chem. Soc. 116 (1994) 2859.
[37] J.E. Hux, R.J. Puddephat, J. Organomet. Chem. 437 (1992) 251.
[38] K. Kaupp, H. Stoll, W. Kaim, T. Stahl, G. van Koten, E. Wissing, W.J. Smeets, A.L. Spek, J. Am. Chem. Soc. 113 (1991) 5606.
[39] G.J. Stor, S.L. Morrison, D.J. Stufkens, A. Oskam, Organometallics 13 (1994) 2641.
[40] C.J. Kleverlaan, F. Hartl, D.J. Stufkens, J. Photochem. Photobiol. 203 (1997) 231.
[41] C.J. Kleverlaan, D.J. Stufkens, Eur. J. Inorg. Chem., in press.
[42] M.J.A. Kraakman, K. Vrieze, H. Kooijman, A.L. Spek, Organometallics 11 (1992) 3760.
[43] H.J. Huhn, S.E. Braslavsky, R. Schmidt, Pure Appl. Chem. 61 (1989) 187.
[44] H.G. Heller, J.R. Langan, J. Chem. Soc. Perkin Trans. 2 (1981) 341.
[45] J. Víchová, F. Hartl, A. Vlček Jr., J. Am. Chem. Soc. 114 (1992) 10903.
[46] D.M. Manuta, A.J. Lees, Inorg. Chem. 25 (1986) 1354.
[47] J. Reinhold, R. Benedix, P. Birner, H. Hennig, Inorg. Chim. Acta 33 (1979) 209.
[48] H.A. Nieuwenhuis, D.J. Stufkens, R.-A. McNicholl, A.H.R. Al-Obaidi, C.G. Coates, S.E.J. Bell, J.J. McGarvey, J. Westwell, M.W. George, J.J. Turner, J. Am. Chem. Soc. 117 (1995) 5579.

[49] G.J. Stor, F. Hartl, J.W.M.v. Outersterp, D.J. Stufkens, Organometallics 14 (1995) 1115.
[50] H. tom Dieck, W. Rohde, U. Behrens, Z. Naturforsch. 44b (1989) 158.
[51] S. Terabe, K. Kuruma, R. Konaka, J. Chem. Soc. Perkin 2 (1973) 1252.
[52] A. Rosa, G. Ricciardi, E.J. Baerends, D.J. Stufkens, J. Phys. Chem. 100 (1996) 15346.
[53] H.A. Nieuwenhuis, PhD Thesis, University of Amsterdam, 1994.
[54] B.D. Rossenaar, F. Hartl, D.J. Stufkens, Inorg. Chem. 35 (1996) 6194.
[55] T. van der Graaf, R.M.J. Hofstra, P.G.M. Schilder, M. Rijkhof, D.J. Stufkens, J.G.M. van der Linden, Organometallics 10 (1991) 3668.